Bull. Nov. Comp. Center, Num. Anal., 6 (1994), 9–27

Numerical analysis of stochastic auto-oscillating systems*

T.A. Averina, S.S. Artemiev, H. Schurz

The paper considers the questions of the numerical analysis of stochastic auto-oscillating systems. The low computer costs variable stepsize algorithms was constructed for solving the non-linear stochastic differential equations. There are given results of numerical experiments obtained with the help of the dialogue system "Dynamics and Control".

1. Introduction

In recent years the chaotic oscillations in dynamic systems of different nature have raised considerable interest among physicists and mathematicians [1, 2]. Since the determinate chaos is observed in the non-linear systems of the Ordinary Differential Equations (ODEs) when their dimension is $N \geq 3$, obviously, the role of numerical simulation in analyzing ODEs is rising. Using the classical Runge-Kutta methods of the 4-th order for numerical solution of the auto-oscillating ODEs with a constant integration step may lead to quite improper conclusions about properties of the solution ocsillations of ODEs. The complicated non-regular behaviour of the solution trajectories of such ODEs requires the compulsory presence the estimation of the error of the numerical solution and the procedure of the automatic choice of the integration stepsize in the numerical algorithm. A number of highly effective variable stepsize algorithms for solving ODEs have been constructed by the present time [3, 4].

Random fluctuations affecting the auto-oscillation systems may have principal significance, because they may determine the type of newly established oscillations [2]. Numerical simulation of the oscillating ODEs under the influence of random fluctuations is reduced to statistical simulation of the solution trajectories of the system of non-linear Stochastic Differential Equations (SDEs). As in the determinate case, variable stepsize algorithms for numerical solution of oscillating SDEs are also required.

*Supported by the Russian Foundation of Fundamental Research under Grant 94-01-00074.

The existing variable stepsize algorithm is based on the imbedded 5- and 6-stage generalized Runge-Kutta methods [5]. It is intended for solving problems of the optimal control, where usually there is no need in the simulation of the large number of trajectories. However, for obtaining different probabilistic characteristics of stochastical oscillations the simulation of the large number of trajectories is needed, but it is a time-consuming task. Therefore, the variable stepsize algorithms for solving the stochastical oscillations systems must require low computer costs and in the proposed paper we will construct the generalized 3-stage Runge-Kutta method as the basis for low computer cost variable stepsize algorithms for solving SDEs. The main demand for this algorithm is to provide the possibility of simulating the oscillating trajectories with not high accuracy and with the stable integration stepsize.

Using the interaction system "Dynamics and Control" including the constructed variable stepsize algorithm, numerical experiments on different test SDEs were carried out.

2. Strange attractors, bifurcation, phase transitions

Consider a system of ODEs in the form:

$$\begin{aligned} &\frac{dy(t)}{dt} = f(t, y(t), \mu), \quad t_0 \le t \le t_{\text{end}}, \\ &y(t_0) = y_0, \end{aligned} \tag{1}$$

where f is N-dimensional vector function, $\mu = (\mu_1, \ldots, \mu_k)$ is a vector of real parameters. Throughout the paper we assume that system (1) for a certain μ is auto-oscillating, i.e., it has a *limit cicle*. The limit cicle is a particular case of the *attractor* – a bounded attractive limit set. The attractor which has the non-periodic auto-oscillating mode is called *strange*. Only the auto-oscilating system of $N \ge 3$ dimension can have a strange attractor. The classical example of the system of SDE's with a strange attractor is the Lorence system :

$$\begin{aligned} \frac{dy_1(t)}{dt} &= -\mu_1(y_1 - y_2), \\ \frac{dy_2(t)}{dt} &= \mu_2 y_1 - y_2 - y_1 y_3, \\ \frac{dy_3(t)}{dt} &= -\mu_3 y_3 + y_1 y_2. \end{aligned} \tag{2}$$

With μ continuously changing along some curve γ in the space of parameters it can be appear that in passing some points on this curve the qualitative rebuilding of the phase portrait takes place. Such values of parameters are called *points of bifurcation* of the phase portrait, and this phenomenon is said to be *the bifurcation*. So μ^* is the point of bifurcation if in an arbitrary small vicinity there are points with qualitatively different phase portraits. The transition from one phase portrait to another with changing the vector of parameters μ is called *the phase transition*. The bifurcation of the strange attractor can exist as phase transition of the types "chaos-chaos" or "chaos-order".

Any movement of real dynamical objects takes place under the influence of random fluctuations. The role of fluctuations gains special importance near the points of bifurcation when even small fluctuations of parameters or exterior noise can initiate various phase transitions. The investigation of influences of random disturbances on a dynamic system usually reduces to the analysis of SDEs

$$dy(t) = f(t, y(t), \mu)dt + \sigma(t, y(t))dw(t), \tag{3}$$

where $\sigma(t, y)$ is a matrix function of $N \times M$- dimension, $w(\cdot)$ is M- dimensional standard Wiener's process. The solution of SDEs has such probabilistic characteristics as mean, the matrix of covariance, the function of correlation, the probability distribution density function. For stationary ergodic random processes the spectral density is also the probabilistic characteristics.

3. Variable stepsize algorithm

Let the s-stage Runge-Kutta method for solving ODEs (1) has the form:

$$\begin{aligned} y_{n+1} &= y_n + \sum_{i=1}^{s} p_i k_i, \\ k_i &= hf(t_n + c_i h, y_n + \sum_{j=1}^{i-1} \beta_{ij} k_j, \mu), \quad i = 1, \ldots, s, \\ \beta_{10} &= 0, \quad c_i = \sum_{j=1}^{i-1} \beta_{ij}, \quad i = 2, \ldots, s, \end{aligned} \tag{4}$$

where p_i, $\beta_{i,j}$ are the coefficients of this method, y_n is a numerical solution at the mesh node t_n, h is the integration step at the mesh node t_n. It can be generalized for the solution of SDEs in the sense of Ito (3) in the following way:

$$y_{n+1} = y_n + \sum_{i=1}^{s} p_i k_i + \sqrt{h}\sigma(t_n, y_n)\zeta_n, \tag{5}$$

where ζ_n are M-dimensional random vector of independent standard Gaussian components. More detailed description of the various families of numerical methods for solving SDEs may be found, for example, in [6,7,8].

The Taylor expansion of the numerical solution (5) in the neighbourhood of the point t_n on a uniform mesh has the form:

$$y_{n+1} = y_n + \sqrt{h}\sigma(t_n, y_n)\zeta_n + hf(t_n, y_n, \mu) + C(h), \tag{6}$$

and for the moments of the remainder term $C(h)$ are valid the following asymptotic behaviour:

$$\langle C(h)\rangle = O(h^2), \quad \langle C^2(h)\rangle = O(h^3)$$

as $h \to 0$. Here $\langle\cdot\rangle$ denotes the mean operation. Comparing the Taylor expansion (6) with the Taylor expansion of the exact solution of SDEs in the sense of Ito [7] we see at once that numerical methods (5) have the first order of convergence in the meansquare for arbitrary SDEs and have the second order – for SDEs with a constant matrix σ.

The well-known imbedded Runge–Kutta–Fehlberg methods of the second and third order for solving ODEs (1) have the form [4]:

$$\begin{aligned} &y_{n+1} = y_n + \frac{1}{6}(k_1 + k_2 + 4k_3), \quad y^*_{n+1} = y_n + \frac{1}{2}(k_1 + k_2), \\ &k_1 = hf(t_n, y_n, \mu), \\ &k_2 = hf(t_n + h, y_n + k_1, \mu), \\ &k_3 = hf\Big(t_n + \frac{h}{2}, y_n + \frac{1}{4}(k_1 + k_2), \mu\Big), \end{aligned} \tag{7}$$

where y_{n+1} is a numerical solution at the point t_{n+1} which is obtained by the method of the 3-rd order, y^*_{n+1} is a numerical solution at the point t_{n+1} which is obtained by the method of the second order. According to (5) the following methods are the generalization (7) for solving SDEs in the sense of Ito:

$$\begin{aligned} y_{n+1} &= y_n + \frac{1}{6}(k_1 + k_2 + 4k_3) + \sqrt{h}\sigma(t_n, y_n)\zeta_n, \\ y^*_{n+1} &= y_n + \frac{1}{2}(k_1 + k_2) + \sqrt{h}\sigma(t_n, y_n)\zeta_n. \end{aligned} \tag{8}$$

Variable stepsize algorithms automatically choose a stepsize so that the local error of the methods should not exceed the given quantity ϵ. The

following choice procedure of the integration stepsize is used in the variable stepsize algorithms for ODEs (1) based on methods (7) [4].

If h is the chosen initial step at the point t_n, then y_{n+1} and y^*_{n+1} are calculated with this step. Then estimation of the error of the numerical solution at the node t_{n+1} is calculated by the formula:

$$\delta_{n+1} = \left(\frac{1}{N} \sum_{i=1}^{N} \left(\frac{y^*_{n+1,i} - y_{n+1,i}}{d_i} \right)^2 \right)^{1/2}, \tag{9}$$

where the scaling factor is equal to $d_i = \max\{1, |y_{n+1,i}|, |y_{n,i}|\}$. The obtained estimation δ_{n+1} is compared to ϵ, which allows us to predict the optimal stepsize

$$h_{\text{new}} = \frac{h}{\max\{r_1, \min\{r_2, (\frac{\delta_{n+1}}{\epsilon})^{1/3}/r\}\}}, \tag{10}$$

where $r = 0.9$ is a guaranteed factor which is used for the estimation in the nearest mesh node be admissible with high probability. The coefficient of maximum increasing the step is set as $r_1 = 0.1$ and the coefficient of minimum decreasing the step is set as $r_2 = 5$. The step from t_n to t_{n+1} is assumed successful, if

$$\delta_{n+1} \leq \epsilon, \tag{11}$$

and for further calculation from the mesh node t_{n+1} to t_{n+2} the integration stepsize is chosen according to (10). If inequality (11) is untrue then the return is done and the integration from the mesh node t_n to t_{n+1} is realized with the integration stepsize h_{new} according to (10)

This procedure of the choice of the integration step is transferred to solving SDEs in the sense of Ito (3) with inconsiderable change: instead of inequality (11) the inequality

$$\delta_{n+1} \leq 5\epsilon \tag{12}$$

is verified. The fluctuations of the numerical solution at the expense of the diffusion term in the error estimation (9) are not taken into account, as

$$y_{n+1} - y^*_{n+1} = -\frac{1}{3}(k_1 + k_2 - 2k_3).$$

Method (7) can be generalized for the solution of SDEs in the sense of Stratonovich in the following way:

$$y_{n+1} = y_n + \frac{1}{6}(k_1 + k_2 + 4k_3) + \sqrt{h}(2G_3 - G_1)\zeta_n, \tag{13}$$
$$G_1 = \sigma(t_n, y_n),$$
$$G_2 = \sigma\Big(t_n, y_n + \frac{6}{5}k_1 + \frac{1}{2}G_1\sqrt{h}\zeta_n\Big),$$
$$G_3 = \sigma\Big(t_n + \frac{h}{2}, y_n + \frac{1}{4}(k_1 + k_2) + \frac{1}{24}(G_1 + 5G_2)\sqrt{h}\zeta_n\Big),$$

where k_i are the same as in (7). This numerical methods (13) have the first order of convergence in the meansquare for arbitrary SDEs and have the second order – for SDEs with a constant matrix σ. The procedure of the estimation of the error and the choice of the integration step for solving SDEs in the sense of Ito is transferred to solving SDEs in the sense of Stratonovich without change.

4. Models and numerical experiments

Numerical experiments were made on PC/AT 486DX-2 using the Dialogue System (DS) "Dynamics and Control". It is worked out at the Computing Center of Sibirian Division of the Russian Academy of Sciences, Nonosibirsk, Russia. It is intended for numerical experiments when solving the problems of analysis and synthesis of automatic control of dynamical objects.

The DS has the following algorithms of statistical simulation of the solution of SDE:

- the Euler-Maruyama method for SDEs in the sense of Ito;
- the generalized two-stage Runge-Kutta method for SDEs in the sense of Stratonovich;
- the generalized one-stage Rosenbrock type methods for SDEs in the sense of Ito;
- the generalized two-stage Rosenbrock type method for SDEs in the sense of Ito and Stratonovich;
- the Mil'shtein method for SDEs in the sense of Ito with single noise;
- the Platen method for SDEs in the sense of Ito with single noise;
- the Newton methods for SDEs in the sense of Ito and Stratonovich with single noise;
- two variable step algorithms for SDEs in the sense of Ito and Stratonovich.

The DS allows one to evaluate the following functionals of SDEs solutions:

- mean;
- covariance matrix;
- correlation function of a required component of the solution;
- distribution density of a required component of the solution;
- spectral density of a required component of the solution;
- joint distribution density of two required components of the solution;
- two-dimensional distribution density of a required component of the solution at two required grid points.

Numerical tests of the constructed algorithm of the variable step were conducted for stochastic dynamical systems with strange attractors. A preliminary attempt was made to calculate such systems with the help of various numerical methods with the constant step failed because of the overflow even by using very small stepsizes.

All examples given bellow are taken from [1, 2]. Each ODEs was solved by the algorithm of the variable step RKF45 constructed on the basis of the imbedded 5-and 6-stage Runge–Kutta–Fehlberg methods [3]. Parameters of ODEs are chosen so that the solution of the system has complex non-regular oscillations. Then the solution of SDEs in the sense of Ito obtained from ODEs with the "noising" parameters was simulated with the help of the constructed algorithm of the variable step. In all the examples the initial value of SDEs solution was the normal random vector with independent components, having the same variance $D = 0.01$, and the demanded accuracy of calculations was equal to $\epsilon = 10^{-3}$. Main objectives of the numerical experiments are to demonstrate the possibility of the constructed variable step algorithm to simulate the SDEs solution with complex oscillating character and to show what happens with SDEs solution if parameters of the system start to "noise".

Example 1. Auto-oscillations in the generator with inertial non-linearity are:

$$\begin{aligned} \frac{dy_1(t)}{dt} &= y_2 + \mu_1 y_1 - y_1 y_3, \\ \frac{dy_2(t)}{dt} &= -y_1, \\ \frac{dy_3(t)}{dt} &= \mu_2(-y_3 + \lambda(y_1)y_1^2), \end{aligned} \tag{14}$$

where $\lambda(y)$ is the Heviside function:

$$\chi(y) = \begin{cases} 1, & \text{at} \quad y > 0, \\ 0, & \text{at} \quad y \leq 0. \end{cases}$$

The change of a phase portrait at the account of high intensity of the noise of the parameters μ can be observed in Figures 1 and 2.

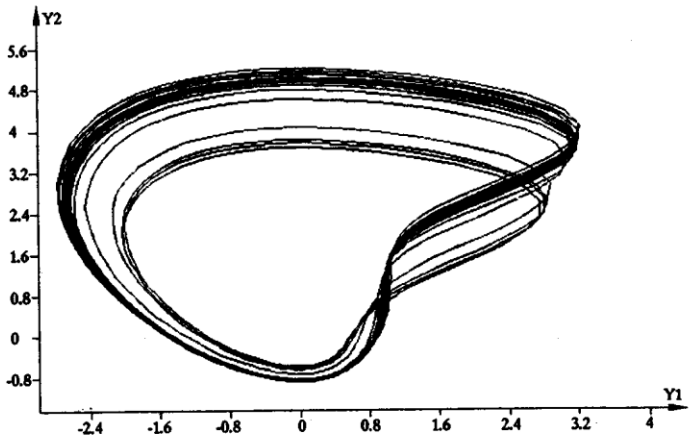

Figure 1. Phase trajectory (y_1, y_2) at $\mu_1 = 1.09$, $\mu_2 = 0.9$ (noise is absent)

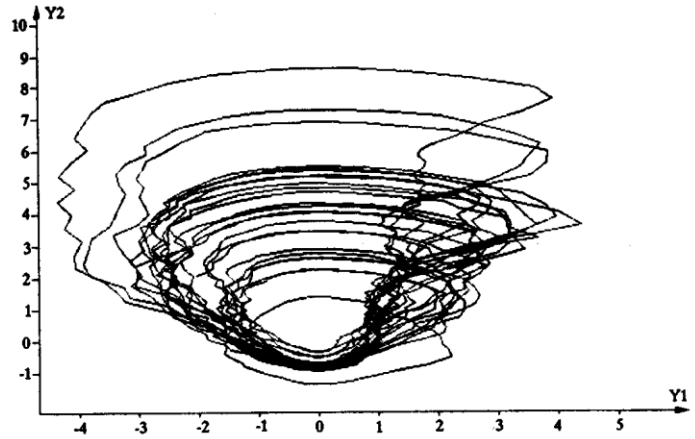

Figure 2. Phase trajectory (y_1, y_2) at $\mu_1 = 1.09 + 0.2\frac{dw_1}{dt}$, $\mu_2 = 0.9 + 0.2\frac{dw_2}{dt}$

One trajectory of the SDEs solution in the interval [0,200] on the grid having 2000 nodes was simulated. The number of the algorithm steps is equal to 2346 at the inessential noise and 2412 – at the intensive noise. There were not fixed any wrongly predicted sizes of the integration step.

Figure 3 presents a graph of evaluating the spectral density of the component y_1 of the SDEs solution (14), when

$$\mu_1 = 1.45 + 0.01\frac{dw_1}{dt}, \quad \mu_2 = 0.3 + 0.01\frac{dw_2}{dt}.$$

At such parameters the SDEs has a strange attractor and continuous spectrum of the solution.

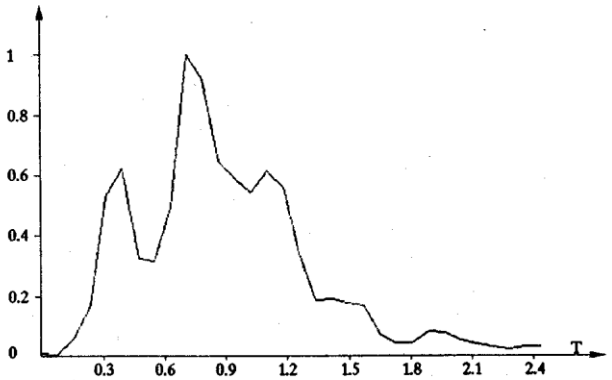

Figure 3. Spectral density of the first component of the solution (14)

Example 2. A system of the Lorenz equations (2) is a simple three-mode model of the convective turbulence. Assume that in system (2) the parameters $\mu_1 = 10$, $\mu_3 = \frac{8}{3}$, and the parameter μ_2 is "noising".

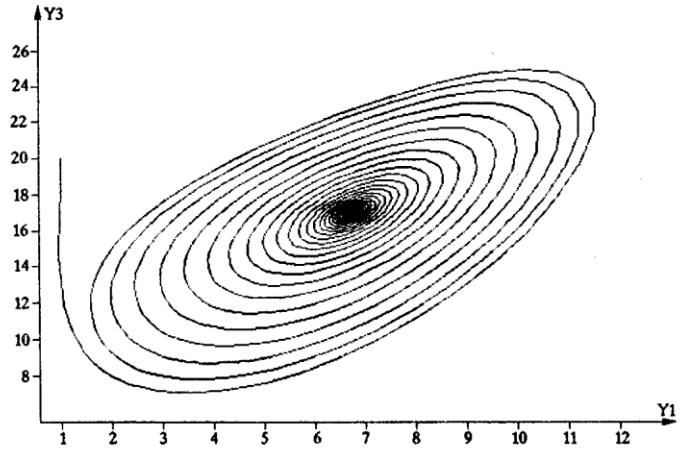

Figure 4. Phase trajectory (y_1, y_3) at inessential noise

In this example high intensity of the noise of the parameter μ_2 brings about the qualitative change of the phase portrait. Figure 4 shows the phase trajectory (y_1, y_3) of the SDEs solution (2) at $\mu_2 = 18 + 0.04\frac{dw_1}{dt}$, and Figure 5 – at $\mu_2 = 18 + 0.4\frac{dw_1}{dt}$.

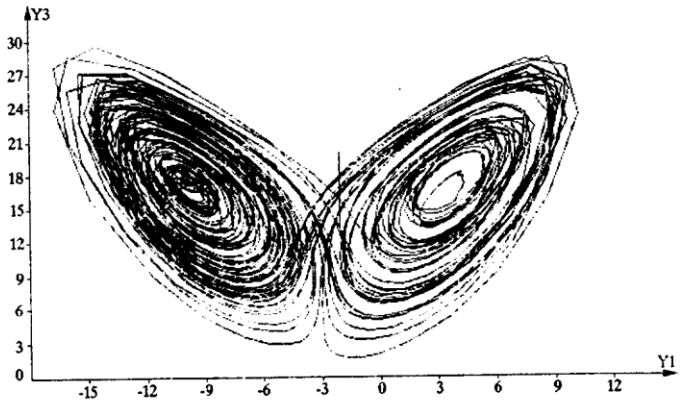

Figure 5. Phase trajectory (y_1, y_3) at the intensive noise

As is seen, SDEs (2) has a regular attractor at the inessential noise and a strange attractor at the intensive noise. One trajectory of the SDEs solution in the interval [0,100] on the grid having 2000 nodes was simulated. The number of the algorithm steps is equal to 2330 at the inessential noise and 4603 – at the intensive noise. There were not fixed any wrongly predicted sizes of the integration step.

Example 3. A system of the Rössler equations

$$\begin{aligned} \frac{dy_1(t)}{dt} &= -y_2 - y_3, \\ \frac{dy_2(t)}{dt} &= y_1 + \mu_1 y_2, \\ \frac{dy_3(t)}{dt} &= \mu_2 + y_1 y_3 - \mu_3 y_3 \end{aligned} \tag{15}$$

describes a hypothetic chemical reaction. Figure 6 presents the phase trajectory (y_1, y_3) of the ODEs solution (15) at $\mu_1 = 0.2$, $\mu_2 = 0.2$, $\mu_3 = 2.83$. Figure 7 presents a graph of the joint density of the first and the second components of the SDEs solution (15) with the following noising parameters:

$$\mu_1 = 0.2 + 0.01\frac{dw_1}{dt}, \quad \mu_2 = 0.2 + 0.01\frac{dw_2}{dt}, \quad \mu_3 = 2.83 + 0.1\frac{dw_3}{dt}.$$

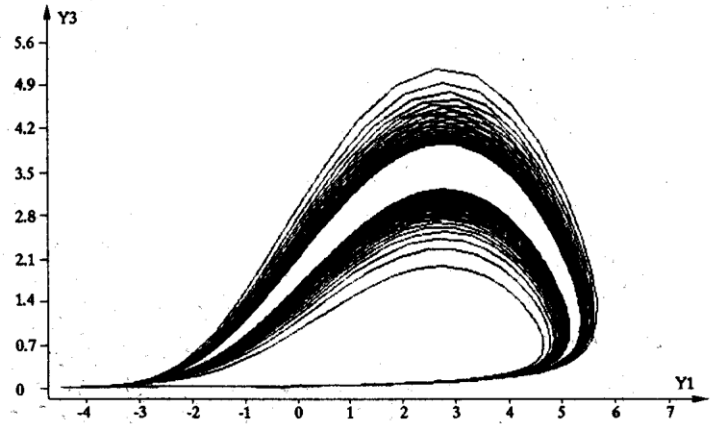

Figure 6. Phase trajectory (y_1, y_3)

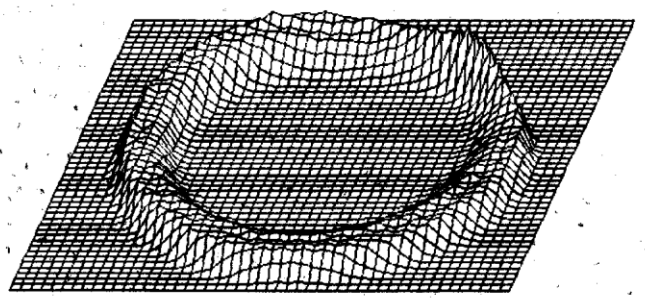

Figure 7. Graph of the joint density

The estimation of the joint density is obtained along one trajectory of the SDEs solution in the interval [0,20000] on the grid having $2*10^5$ nodes. The number of the algorithm steps is equal to 266750. There were not fixed any wrongly predicted sizes of the integration step. With increasing the intensity of the noise of parameters in the algorithm, the integration step size can decrease up to the computer zero, and simulation of the problem terminates with the message: "The demanded accuracy of computation is not attained".

Figure 8 presents a graph of the estimation of the spectral density of the component y_1 of SDEs solution at

$$\mu_1 = 0.3 + 0.001\frac{dw_1}{dt}, \quad \mu_2 = 0.4 + 0.001\frac{dw_2}{dt}, \quad \mu_3 = 8.5 + 0.001\frac{dw_3}{dt}.$$

With these parameters SDEs (15) has a strange attractor.

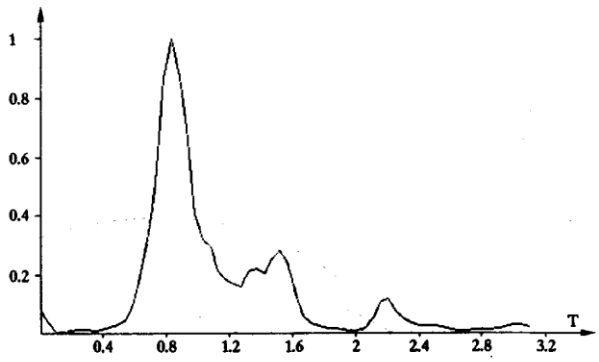

Figure 8. Spectral density

Example 4. Two connected brusselators

$$\begin{aligned}
\frac{dy_1(t)}{dt} &= \mu_1 - 5.56y_1 + y_1^2 y_3 + \mu_2(y_2 - y_1),\\
\frac{dy_2(t)}{dt} &= \mu_3 - 3.308y_2 + y_2^2 y_4 + \mu_2(y_1 - y_2),\\
\frac{dy_3(t)}{dt} &= 4.56y_1 - y_1^2 y_3 + \mu_2(y_4 - y_3),\\
\frac{dy_4(t)}{dt} &= 2.308y_2 - y_2^2 y_4 + \mu_2(y_3 - y_4)
\end{aligned} \tag{16}$$

describe concentration oscillations of responding substances in a chemical reaction. At constant parameters $\mu_1 = 1.6$, $\mu_2 = 0.125$, $\mu_3 = 0.555$ the phase trajectory (y_2, y_4) of the SDEs solution (16) is of the form presented in Figure 9.

Figure 10 shows for component y_3 of the SDEs solution (16) a graph of estimation of the correlation function $R(t, t+\tau)$ at the point $t = 10$, obtained at the following noising parameters:

$$\mu_1 = 1.6 + 0.1\frac{dw_1}{dt}, \quad \mu_2 = 0.125 + 0.1\frac{dw_2}{dt}, \quad \mu_3 = 0.555 + 0.1\frac{dw_3}{dt}.$$

The correlation function estimation is obtained by the simulation of an ensemble of 100 trajectories of the SDEs solution (16) in the interval [0,20] on the grid having 200 nodes. The total number of steps of the algorithm is equal to 33563. 21 wrongly predicted integration step sizes were fixed in the course of computation.

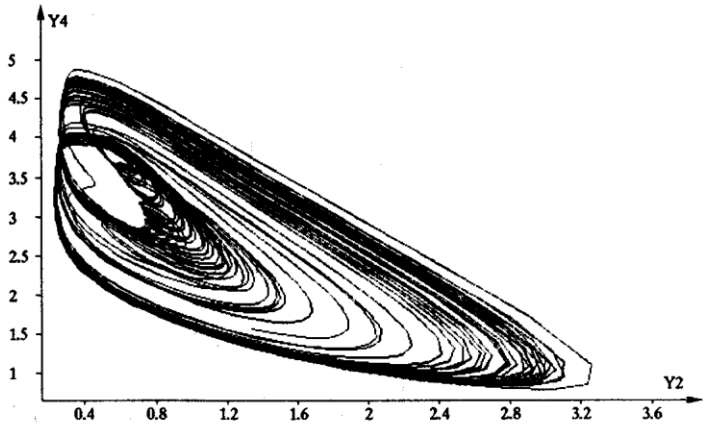

Figure 9. Phase trajectory (y_2, y_4)

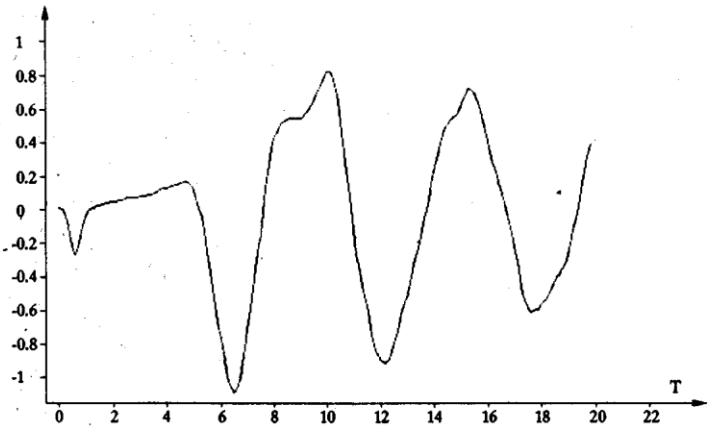

Figure 10. Graph of the correlation function

Example 5. A seven-dimensional discrete model of the Navier-Stokes equation, as a system of the Lorenz equations, describes the convective turbulence:

$$\begin{aligned}
\frac{dy_1(t)}{dt} &= -2y_1 + \mu_1(y_2y_3 + y_4y_5),\\
\frac{dy_2(t)}{dt} &= -9y_2 + \mu_2(y_1y_3 + y_6y_7),\\
\frac{dy_3(t)}{dt} &= -5y_3 + \mu_3y_1y_7 - 7\sqrt{5}y_1y_2 + \mu_6,\\
\frac{dy_4(t)}{dt} &= -5y_4 - \sqrt{5}y_1y_5,
\end{aligned} \tag{17}$$

$$\frac{dy_5(t)}{dt} = -y_5 - \mu_4 y_1 y_4,$$
$$\frac{dy_6(t)}{dt} = -8y_6 - 4\sqrt{5}y_2 y_7,$$
$$\frac{dy_7(t)}{dt} = -5y_7 + \sqrt{5}y_2 y_6 - \mu_5 y_1 y_3,$$

where μ_6 is an analogy with Reinold's number. Figure 11 presents the phase trajectory (y_3, y_5) of the ODEs solution (17) at the following parameters: $\mu_1 = 4\sqrt{5}$, $\mu_2 = 3\sqrt{5}$, $\mu_3 = 9$, $\mu_4 = 3\sqrt{5}$, $\mu_5 = 9$, $\mu_6 = 360$.

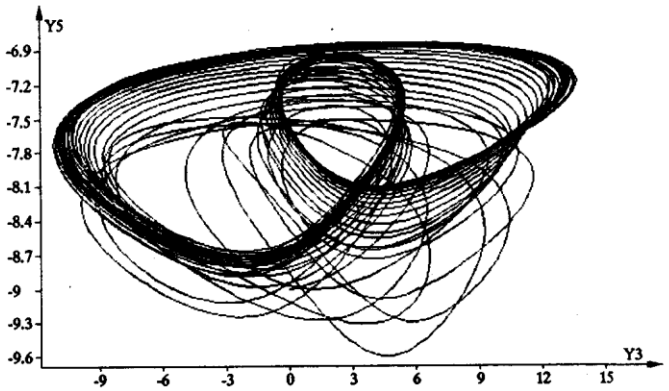

Figure 11. Phase trajectory (y_3, y_5)

Six noising parameters will be set in the following manner:

$$\mu_1 = 4\sqrt{5} + 0.001\frac{dw_1}{dt}, \quad \mu_2 = 3\sqrt{5} + 0.001\frac{dw_2}{dt}, \quad \mu_3 = 9 + 0.001\frac{dw_3}{dt},$$
$$\mu_4 = 3\sqrt{5} + 0.001\frac{dw_4}{dt}, \quad \mu_5 = 9 + 0.001\frac{dw_5}{dt}, \quad \mu_6 = 360 + 0.1\frac{dw_6}{dt}.$$

Figure 12 presents a graph of the joint density estimation of the third and the fifth components of the SDEs solution (17), and Figure 13 – one-dimensional density of the third component.

Density estimations are obtained along one trajectory of the SDEs solution in the interval [0,500] on the grid having 2×10^5 nodes. There were no difficulties in the numerical simulation. The number of steps of the algorithm is equal to 379766, no wrongly predicted integration step size was fixed. For testing the procedure of changing the integration step size, similar calculations for the high noise intensity of parameters:

$$\mu_1 = 4\sqrt{5} + 0.1\frac{dw_1}{dt}, \quad \mu_2 = 3\sqrt{5} + 0.1\frac{dw_2}{dt}, \quad \mu_3 = 9 + 0.1\frac{dw_3}{dt},$$
$$\mu_4 = 3\sqrt{5} + 0.1\frac{dw_4}{dt}, \quad \mu_5 = 9 + 0.1\frac{dw_5}{dt}, \quad \mu_6 = 360 + \frac{dw_6}{dt}$$

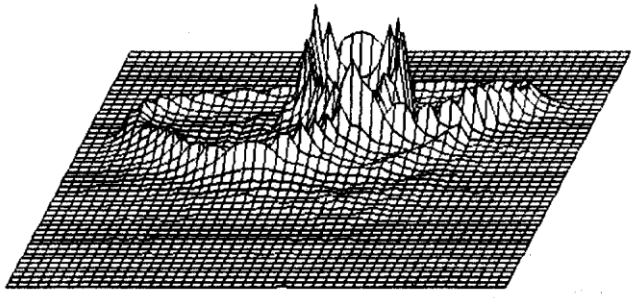

Figure 12. Graph of the joint density

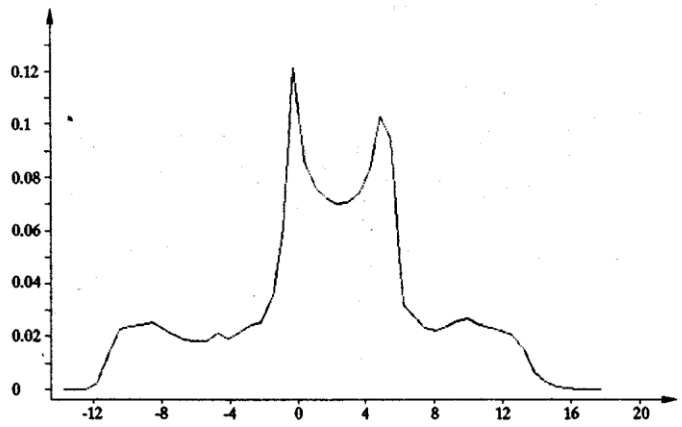

Figure 13. Graph of the one-dimensional density

were carried out. The number of steps has increased up to 427068 and 22 wrongly predicted integration step sizes were fixed.

Example 6. A model of three-wave resonance interaction describes the combinative light scattering in the dielectric:

$$\begin{aligned} \frac{dy_1(t)}{dt} &= y_1 - \mu_1 y_2 + y_2(y_3 + y_1^2), \\ \frac{dy_2(t)}{dt} &= y_2 + \mu_1 y_1 + y_1(3y_3 - y_1^2), \\ \frac{dy_3(t)}{dt} &= -\mu_2 y_3 - 2y_1 y_2 y_3. \end{aligned} \tag{18}$$

Figure 14 presents the phase trajectory (y_2, y_3) of the SDEs solution (18) for the parameters: $\mu_1 = 1.15$, $\mu_2 = 2.52$.

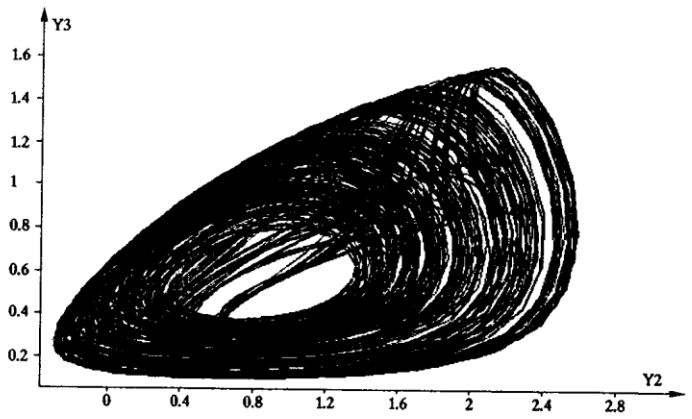

Figure 14. Phase trajectory (y_2, y_3)

Figure 15 presents a graph of the integral curve $y_1(t)$ of the SDEs solution (18) for the case of "weakly noising" parameters:

$$\mu_1 = 1.15 + 0.0001\frac{dw_1}{dt}, \quad \mu_2 = 2.52 + 0.001\frac{dw_2}{dt},$$

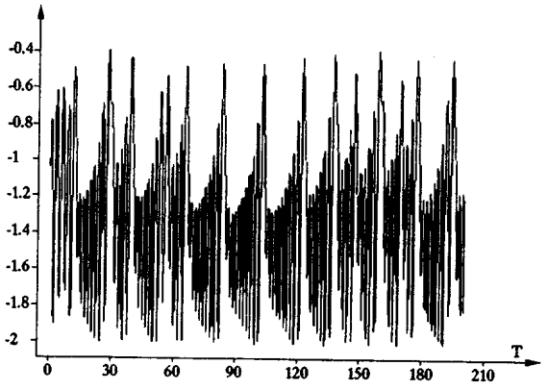

Figure 15. Graph of the integral curve $y_1(t)$ at the inessential noise

Figure 16 – for the case of "intensively noising" parameters:

$$\mu_1 = 1.15 + 0.1\frac{dw_1}{dt}, \quad \mu_2 = 2.52 + 0.1\frac{dw_2}{dt}.$$

Integral curves are obtained at the simulation of the trajectory of the SDEs solution (18) in the interval [0,200] on the grid having 2000 nodes. The number of steps of the algorithm at the inessential noise is equal to 3785. At the intensive noise we failed to do simulation due to decreasing the integration step size up to the computer zero.

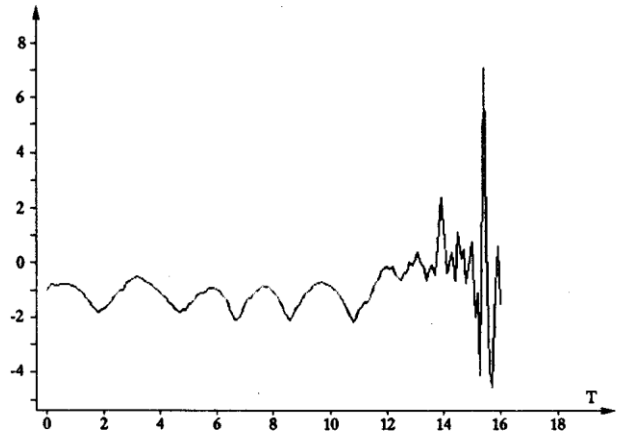

Figure 16. Graph of the integral curve $y_1(t)$ at the intensive noise

Example 7. In a model of the ecological system "plunderer – victim"

$$\begin{aligned}
\frac{dy_1(t)}{dt} &= -\mu_1 y_1 - 2\frac{y_1 y_2}{1+0.08y_1} + \frac{y_1 M_0}{1+0.08M_0},\\
\frac{dy_2(t)}{dt} &= -\mu_1 y_2 + \frac{y_1 y_2}{1+0.08y_1},\\
\frac{dy_3(t)}{dt} &= -\mu_2 y_3 - 2\frac{y_3 y_4}{1+0.08y_3} + \frac{y_3 M_0}{1+0.08M_0},\\
\frac{dy_4(t)}{dt} &= -\mu_2 y_4 + \frac{y_3 y_4}{1+0.08y_3},
\end{aligned} \tag{19}$$

where M_0 is the quantity of the biogenic element: $M_0 = 20 - y_1 - y_2 - y_3 - y_4$, y_1 and y_3 are the biogenic contents in victims, y_2 and y_4 are the biogenic contents in plunderers. Figure 17 presents the phase trajectory (y_3, y_4) of the ODEs solution (19) at the following parameters: $\mu_1 = 1$, $\mu_2 = 2$.

Two noising parameters of the system will be given as follows:

$$\mu_1 = 1 + 0.1\frac{dw_1}{dt}, \quad \mu_2 = 2 + 0.1\frac{dw_2}{dt}.$$

Figure 18 presents a graph of estimation of the correlation function $R(t, t+\tau)$ of the third component of the SDEs solution (19).

Estimation of the correlation function is obtained at the simulation of 200 trajectories of the SDEs solution (19) on the interval [0,10] on the grid with 80 nodes. The total number of steps of the algorithm is egual to 38245. Three wrongly predicted integration step sizes were fixed in the course of computation.

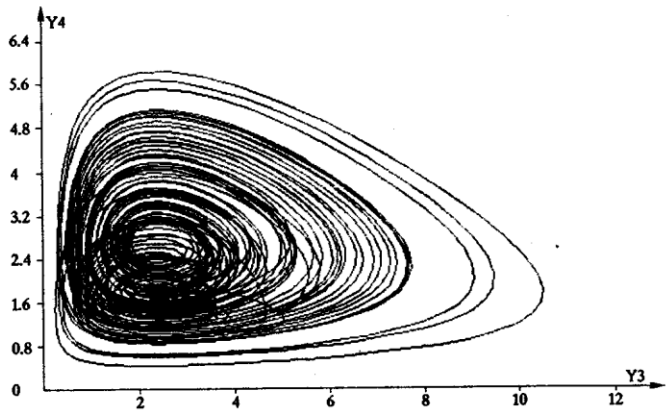

Figure 17. Phase trajectory (y_3, y_4)

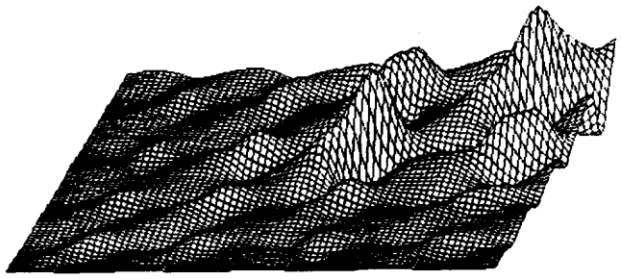

Figure 18. Correlation function

Based on the results of numerical experiments we can come to the conclusion of the high efficiency of the variable step algorithm as applied to statistical simulation of auto-oscillating stochastic systems.

References

[1] U. Neimark, P.S. Landa, *Stochastic and chaos oscillating*, Nauka, Moscow, 1987 (in Russian).

[2] V.S. Anischenko, *Complicated oscillation in simple systems. Mechanisms of occurrence, structure and properties of the dynamic chaos in radio-physical systems*, Nauka, Moscow, 1990 (in Russian).

[3] G.E. Forsythe, M.A. Malcolm, C.B. Mouler, *Computer methods for mathematical calculations*, Englewood Chiffs: Prentice-Hall, 1977.

[4] E. Hairer, S.P. Norsett, G. Wanner, *Solving ordinary differential equations I. Nonstiff problems*, Springer-Verlag, Berlin, Heidelberg, 1987.

[5] T.A. Averina, S.S. Artemiev, *Numerical simulating in problems of analysis and synthesis of stochastic control systems*, Novosibirsk, Computing Center, preprint No. 915, 1990 (in Russian).

[6] S.S. Artemiev, *Numerical Solution of the Cauchy Problem for Systems of Ordinary and Stochastic Differential Equations*, Computing Center SD RAS, Novosibirsk, 1993.

[7] P.E. Kloeden, E. Platen, *The Numerical Solution of Stochastic Differential Equations*, Springer, Berlin-Heidelberg-New-York, 1992.

[8] P.E. Kloeden, E. Platen, H. Schurz, *The Numerical Solution of Stochastic Differential Equations through Computer Experiments*, Springer, Berlin-Heidelberg-New-York, 1994.